Appendix 1 – Analytical Methods

SEM/EPMA

Initial scanning electron microscopy (SEM) analysis was conducted using a Quanta 450 field emission gun (FEG) SEM with silicon-drift detector (Adelaide Microscopy, University of Adelaide). Operating conditions used were 60 Pa chamber pressure, 20 keV accelerating voltage, 0° tilt, 10-11 mm working distance, with a spot size of 4-5.

Subsequent quantitative analysis of the uraninite composition was measured using a Cameca SX-Five electron probe microanalyzer (EPMA) equipped with 5 tunable wavelength-dispersive spectrometers. For spot analyses, operating conditions included a 15 keV accelerating voltage, 100 nA beam current, 40° takeoff angle, with 0.5 to 1 μm-sized beam. A total of 28 elements were measured: U, Pb, Th, Na, Mg, Al, Si, P, S, K, Ca, Ti, Mn, Fe, Cu, As, Zr, Nb, Y, Ce, La, Pr, Nd, Sm, Gd, Sr, Ba, Te. The total acquisition time per point was 9 minutes 42 seconds. Elemental mapping was performed at 20 keV accelerating voltage, 100 nA beam current and 1 μm beam-size. A total of 13 elements were also mapped, with wavelength dispersive spectroscopy (WDS) being used for Ce Lα, P Kα, Ca Kα, Y Lα, and Pb Mα. Energy dispersive spectroscopy (EDS) was used to measure Si Kα, Fe Kα, U Lα, S Kα, Cu Kα, La Lα, Nd Lα, and Ti Kα. Further details of the methodology used for both point analysis and elemental mapping is outlined in Macmillan et al. (2016), as are all details of the standards used, measured element X-ray lines, estimates of minimum detection limits, and mean precision.

Sample Preparation

Surface sample preparation is important for any electron back-scatter diffraction (EBSD) work since it is a surface sensitive technique and analysis is conducted in the top 10-50 nm region of the specimen (Wright et al. 2011). Thus, scratches caused by mechanical polishing and any oxide layers need to be removed prior to EBSD analysis, otherwise poor quality EBSD patterns will be obtained. Standard petrographic thin sections were prepared by Adelaide Petrographic Laboratories with additional polishing/cleaning steps to ensure optimal sample preparation. Preparation steps included:

- Impregnate drill-core rock sample with araldite GY191 and Hardener HY951 and then remove cured araldite from surface using 1200 grit fixed media (wet and dry sand paper).
- Polish sample on ceramic lap with 6 μm diamond paste for 2 to 10 minutes as needed.
- Polish sample using textmet (Buehler textmet 1500 8" PSA) cloth lap with 3 μm diamond paste for 30 – 60 minutes; with 1 μm diamond paste for 40 – 60 minutes; and with 1 or ¼ Kemet WP diamond solution for 30 – 60 minutes.
- Final polish of sample using Struers MD Chem lap Kent polisher with Struers colloidal silica product (OP-S non Dry) for 2 hours.
- Ultrasonic cleaning was also used as required to avoid cross-contamination.

To minimize charging, samples were coated with a 1.5 to 2 nm-thick carbon film via thermal evaporation using a Quorum Q150TE vacuum evaporator. The carbon coat thickness needs to be adequate to prevent surface charging, but not too thick as otherwise only a weak electron diffraction pattern will be observed.

FIB-EBSD

Electron back-scatter diffraction (EBSD) data were collected using the EDAX-TSL™ EBSD system equipped with a Hikari camera on a FEI Helios NanoLab DualBeam™ FIB/SEM platform at Adelaide Microscopy, University of Adelaide.

Samples were mounted onto an analysis stub using Ag-Dag rather than carbon tape which can melt during the long analysis times, causing the sample to move whilst mounted. The mounted sample was then fitted on a 45º tilted sample holder, and was subsequently tilted another 30º, so that the total tilt for analysis was 70º. EBSD patterns were collected at 20 kV and 2.7 nA with a working distance ranging between 10 and 13 mm. The OIM Data Collection (version 5.2) software was used for data collection, and the OIM Analysis (version 4.5) software was used for data analysis and interpretation.

Crystallographic structure files for uraninite (UO_2) were available as part of the standard TSL structural database. Other settings used for EBSD data collection and processing are displayed in Table A1. For the current study, measurement of the UO_2 was of greatest importance, thus all settings and parameters

Table A1: EBSD data collection and processing settings.

General Parameters	
Binned Pattern Size	96
Theta Step Size (degrees)	1
Rho Fraction	90%
Max Peak Count	7
Min Peak Count	3
Hough Parameters	
Hough Type	Classic
Resolution	Low
Convolution Mask	Medium (9x9)
Min Peak Magnitude	5
Min Peak Distance	25
Peak Symmetry	0.7
	S17.12
Grid Type	hexagonal
Working Distance (mm)	13
X Length (μm)	206.5
Y Length (μm)	194.6
Step Size (μm)	0.7
Total Points	95151
Number UO_2 Indexed Points	53875
Average UO_2 CI	0.91
UO_2 Average Fit (degrees)	1.68

(i.e. gain, exposure) were optimized to attain the best possible electron back-scatter pattern (EBSP) for UO_2 rather than any other phase present in the mapped area (i.e., bornite, fluorite).

Since both bornite and fluorite have similar structures to uraninite, and were found in association with the analyzed uraninite grains, another method other than structural differences alone was required for phase identification. Thus EDS chemical data were simultaneously collected and Chemical Indexing (ChI-scan) was conducted after the raw data had been collected, using the procedure outlined by Nowell and Wright (2004). This allowed for individual mineral phases to be identified based on structural and chemical differences.

Once raw data had been collected and imported into the OIM Analysis software, data cleanup was required to minimize the number of incorrectly or non-indexed points and remove noise. Two methods were of relevance for this study: 'Grain CI Standardization' and 'Grain Dilation' (both with grain tolerance angle of 5º and minimum grain size of 2 μm). Grain CI Standardization recovers a portion of the data with a low CI value but the correct orientation. Grain Dilation modifies the orientations of points which do not belong to any grains but have neighboring points which do belong to grains. This method is particularly important for mapping at grain boundaries, where the diffracting volume may be a combination of different crystal lattices and may initially be indexed incorrectly. Data cleanup is a vital part of the data analysis process, but caution must be taken to avoid unnecessary data smoothing that may result in the loss of microstructural detail.

The EBSD data were processed in a number of ways, with Inverse Pole Figure (IPF), Image Quality (IQ) and Grain Reference Orientation Deviation (GROD) mapping being of relevance for the current study. For GROD mapping, each pixel within a grain is colored by the degree of their rotation relative to a reference orientation within the grain. The reference orientation is user-defined, and for the current analysis, the point in the grain with the lowest kernel average misorientation was chosen. Low-angle boundaries have been superimposed on the GROD map (Fig. 2a). These have been defined as being <10º in garnet (Prior et al. 1999), and range between <4 and <10º in zircon (Timms et al. 2006, 2012; Reddy et al. 2007). Thus, low-angle boundaries were defined as <10º for uraninite.

The automated indexing as used by the EBSD system involves matching the measured and theoretical EBSP bands, and there are typically several possible orientations which may satisfy any given pattern. Two methods are typically used to assess the reliability of the automated indexing process, the Confidence Index (CI) or the 'fit' between the measured and theoretical bands. For the uraninite analyzed as part of this study, the average CI was 0.91 and the average band 'fit' for UO_2 was 1.68º. The 'fit' value (often reported as the Mean Angular Deviation) is generally used rather than CI when comparing the quality of EBSD data. Much of the published zircon EBSD data have a 'fit' value of < 1.7º (Timms et al. 2006; Reddy et al. 2007; Moser et al. 2011). Uraninite has not traditionally been analyzed using EBSD, so comparison of this 'fit' value to other published uraninite works was not possible. However, due to the closeness of the average 'fit' value obtained for uraninite measured as part of the current study and that for the published zircon data, the results here were deemed acceptable.

The definition of the legend/coloring used to delineate variation in IQ was critical as if inappropriately defined variability in IQ may not be observed. Thus it would be near impossible to link IQ variation to parameters like chemical variability, porosity or even grain orientation. Numerous iterations of using both color and grayscale to illustrate the variation in IQ were required to clearly display patterns and variability. Thus minor lattice distortion may not be reflected in IQ, and careful definition of the color palette is required to illustrate any possible patterns which reflect variation in microstructure.

APPENDIX 2 – ADDITIONAL FIGURES

Two additional figures are included here, the first of which are pole figures that indicate that the studied zoned uraninite grain (Figs. 1-3) is orientated in the direction (Fig. A1). The second additional figures (Fig. A2) is a supplemental example of another studied uraninite grain (S17.25), highlighting that the relationship between chemical zoning and GROD, as observed for the studied uraninite grain (S17.12), is not atypical.

ADDITIONAL REFERENCES

Moser, D.E., Cupelli, C.L., Barker, I.R., Flowers, R.M., Bowman, J.R., Wooden, J. and Hart, J.R. (2011) New zircon shock phenomena and their use for dating and reconstruction of large impact structures revealed by electron nanobeam (EBSD, CL, EDS) and isotopic U–Pb and (U–Th)/He analysis of the Vredefort dome, Canadian Journal of Earth Sciences, 48, 117-139.

Nowell, M.M. and Wright, S.I. (2004) Phase differentiation via combined EBSD and XEDS, Journal of Microscopy, 213, 296-305.

Timms, N.E., Kinny, P.D. and Reddy, S.M. (2006) Enhanced diffusion of Uranium and Thorium linked to crystal plasticity in zircon. Geochemical Transactions, 7, 1-16.

Timms, N.E., Reddy, S.M., Healy, D., Nemchin, A.A., Grange, M.L., Pidgeon, R.T. and Hart, R. (2012) Resolution of impact-related microstructures in lunar zircon: A shock-deformation mechanism map. Meteoritics & Planetary Science, 47, 120-141.

Wright, S.I., Nowell, M.M. and Field, D.P. (2011) A Review of Strain Analysis Using Electron Backscatter Diffraction, Microscopy and Microanalysis, 17, 316-329.

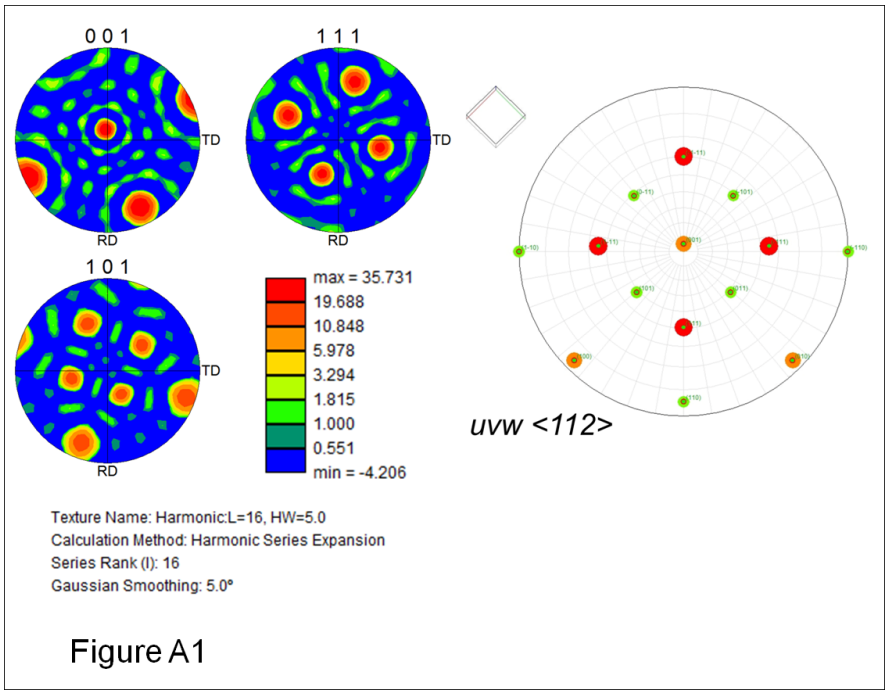

FIGURE A1: Stereographic projections (colored using a logarithmic scale) of crystallographic poles {001}, {110} and {111} of UO_2 for the EBSD data shown in Fig. 1d (uraninite orientation is close to).

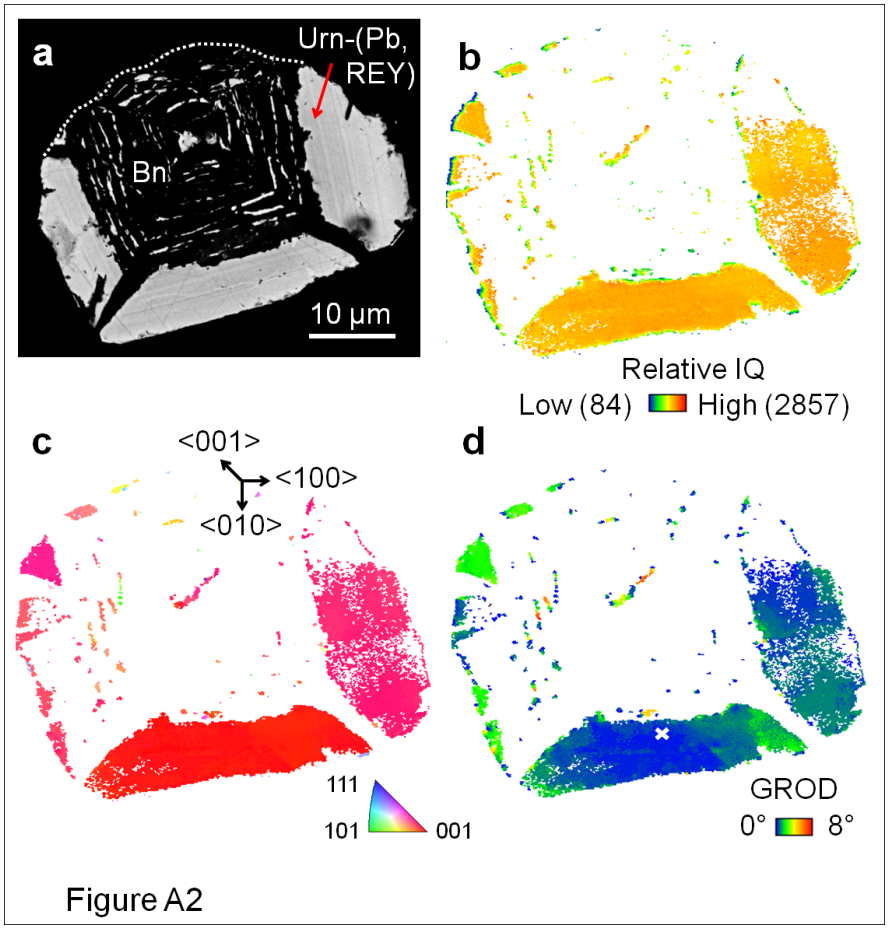

FIGURE A2: SEM- and EBSD-derived images of uraninite grain S17.25 (a) BSE image of uraninite with reduced brightness and contrast to highlight chemical zoning; (b) Image Quality (IQ) map – warmer colors (red-orange) represent areas of higher IQ (higher Pb concentration, low pore/inclusion content), and cooler colors (blue-green) represent areas of lower IQ (edge of grain, lower Pb concentration, higher pore/inclusion content); (c) Inverse Pole Figure (IPF) map of UO_2. UO_2 is of one dominant orientation with some gradational color variation reflecting slight distortion of crystal lattice; (d) Grain Reference Orientation Deviation (GROD) map to show intragrain orientation variations. Each pixel is colored from reference orientation (blue, defined by white cross) with misorientation of up to 8°.